Improvements in time domain FWI and its applications

Kwangjin Yoon, Sang Suh, James Cai and Bin Wang, TGS*

Summary

In this abstract, we describe how to improve time domain full waveform inversion using source wavelet convolution, windowed back propagation and source side illumination. Instead of estimating the source wavelet from field data, a user defined source wavelet can be convolved to field data. This convolution makes waveform matching between modeled and field data easier. Increasing time window applied to residual enables top down velocity update and reduces the possibility of being stuck at a local minimum. The balance of gradient value can be improved by the illumination compensation using the square of source side wavefield. Well balanced gradient helps FWI restore the absolute value of velocity. We apply this method to estimate migration velocities using 2D and 3D synthetic and real data examples.

Introduction

Recently, in seismic imaging, a lot of effort is made to successfully apply Full Waveform Inversion (FWI) to real data, and a few promising results have been gained (Laurent et al., 2011; Lazaratos et al., 2011). FWI seeks to minimize the misfit function between modeled and field data (Tarantola, 1984). To match modeled data to field data, forward modeling may use the source wavelet estimated from field data. In the multi-scale scheme (Bunks et al., 1995), which increases frequency band sequentially, we may use the forward modeling source wavelet as a filter by convolving the source wavelet to modeled and field data. Low frequency wavelet convolution to high frequency data can increase the similarity of waveforms between modeled and field data. Enhanced similarity in waveform can improve FWI convergence.

Migration is a qualitative process. We can control the migration image properly using illumination, simple AGC or scaling after migration. On the other hand, FWI is a quantitative process. In FWI the gradient is calculated using a Reverse Time Migration (RTM) scheme. Because the gradient is based on RTM, FWI is efficient in capturing the geologically relative velocity structure such as reflectivity or velocity gradient which are high frequency friendly. However, reconstructing the absolute value of the velocity is more challenging in FWI because it needs well balanced gradient value. To achieve well balanced gradient in time domain FWI, we compensate the gradient by source side illumination.

The traveltime of signal is usually proportional to the depth where the signal has the information. When we update shallow velocity, we can expect better convergence if we consider signals arriving within the corresponding traveltime because later arriving signals in modeled and field data can contribute to the residual and misfit function. Starting from a small time window, we can update velocity from top to down by increasing the time window. This windowed propagation can reduce the risk of being stuck at a local minimum.

We use the conventional time domain FWI method minimizing the L2 norm of modeled and field data. In the following section, we will describe how to improve time domain FWI using source wavelet convolution to field data, windowed back propagation of residual (Yoon et al., 2003) and source illumination compensation for gradient. Then we will show 2D and 3D synthetic and real data examples which apply time domain FWI to get migration velocities.

Method

The residual is the input for the gradient, and how to compose the residual is the key to the success of FWI. We used low frequency (5Hz~10Hz) Ricker wavelets for forward modeling. The field data was filtered by convolving it with the source wavelet. Figure 1 compares field data (a) before and (b) after 10Hz Ricker wavelet convolution and (c) the modeled data generated using 10Hz Ricker wavelet. The source wavelet convolution to the field data increases similarity between modeled and field data. Increased similarity of waveform can improve the convergence of FWI. In order to implement the multi-scale approach which increases the frequency bandwidth sequentially, modeled and field data were convolved by a Ricker wavelet again. Finally the residual is composed after normalizing modeled and field data by its maximum amplitude.

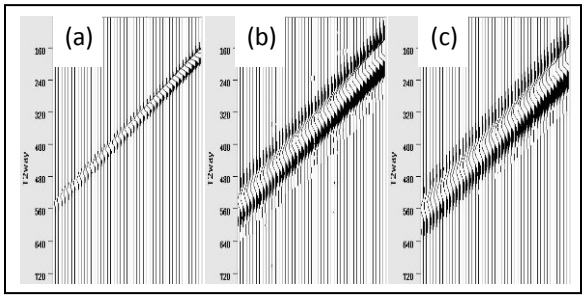

Figure 1. (a) field data, (b) field data after convolving 10Hz Ricker wavelet and (c) modeled data using 10Hz Ricker source wavelet.

In surface seismic data, the recording time of a signal is proportional to the depth of its path. To update the shallow subsurface first and consider the signal generated from the depth, we applied a sequentially increasing time window to the residual. The time window may increase within a frequency band or after swiping the entire frequency band. This is similar approach to the layer stripping velocity update. A layer stripping approach constrains the velocity model. However, windowed back propagation gives a constraint to the residual and the residual produces gradient and misfit function of corresponding depth range.

In implementing the multi-scale scheme, we increased the highest frequency of each frequency band at a constant rate of *frate* as in $freq^{i+1}=frate*freq^{i}$. We used *frate=1.3~1.5.* The updated velocity in FWI can be expressed as a Fourier series of the major frequency of each frequency band. To get a smooth velocity model, FWI needs a smaller *frate.* However, a mild smoothing of gradient and multiple updates of velocity at each frequency band can make the updated velocity smooth.

We calculated the gradient using conventional single shot RTM scheme. To improve the migration velocity using FWI, the

DOI http://dx.doi.org/10.1190/segam2012-1535.1

gradient should be well-balanced because FWI needs to seek the absolute value. The updated velocity cannot be controlled properly after FWI. A few factors influence the balance of RTM-based gradient: 1) Scaling of input as in geometric spreading compensation. 2) Aperture or image muting which can alter the stack count. 3) Illumination compensation using the source or receiver wavefield. 4) Gauss-Newton or full Newton methods in the frequency domain. Because there are many factors, it is difficult to suggest the best workflow. However, empirically speaking, in most cases, the best results have been achieved when we compensated for the geometric spreading and then divided the gradient by the square of the source illumination.

Following Pratt et al.(1998), in the frequency domain, where **d** and **u** are field and modeled data, respectively, the misfit function and the wave equation can be expressed as $E=1/2(\mathbf{d}-\mathbf{u})^2$ and $\mathbf{Su}=\mathbf{f}$. If we consider a wave equation

$$\frac{1}{v^2}\frac{\partial^2 u}{\partial t^2} = \Delta u + f \qquad (1)$$

then the gradient in the frequency domain is given as

$$\frac{\partial E}{\partial v} = \frac{-2}{v^3}\frac{\partial^2 \mathbf{u}}{\partial t^2}\mathbf{S}^{-1}(\mathbf{d}-\mathbf{u})^* \qquad (2)$$

where * denotes the conjugate. Its time domain expression is given as

$$\int_{t=0}^{t=t_{\max}} \frac{-2}{v^3}\frac{\partial^2 S(\mathbf{x},t)}{\partial t^2} R(\mathbf{x},t)\,dt \qquad (3)$$

where $S(\mathbf{x},t)$ is the forward propagating source wavefield and $R(\mathbf{x},t)$ is the back-propagating receiver wavefield whose input is defined as the residual $d(t)$-$u(t)$. We compensated for the geometric spreading of the input and then stacked the gradient in Equation (3) over the total shots and divided the gradient by the square of the total source side illumination of

$$\left\{\sum_{shots}\int_{t=0}^{t=t_{\max}}\left|\frac{-2}{v^3}\frac{\partial^2 S(\mathbf{x},t)}{\partial t^2}\right|dt\right\}^2. \qquad (4)$$

Examples

We tested our FWI with synthetic and real data and produced migration velocities. We tested with synthetic self-generated 2D Marmousi 2 (Martin, 2004) and modified 3D SEG/EAGE data. The same propagator and source wavelet were used for generation of synthetic seismogram and FWI. We did one additional synthetic FWI test with BP2004 original data (Billette and Brandsberg-Dahl, 2005) using the 5Hz Ricker source wavelet. Finally, we applied our FWI to a sequence of 3D marine field data.

Figure 2 shows Marmousi 2 (a) true velocity model, (b) initial velocity model and (c) velocity obtained by FWI. Figure 2 (d), (e) and (f) are RTM images using the velocity models shown in Figure (a), (b) and (c), respectively. The initial velocity was generated by smoothing the true velocity with a 1km*2km moving window of Gaussian weighting function. Synthetic seismograms and FWI used a 10Hz Ricker wavelet. Synthetic seismograms were generated using 100m shot spacing. FWI reconstructed the exact velocity model very well.

Figure 3 shows FWI results on a modified SEG/EAGE velocity model. We added small high velocity (3000m/sec) and low velocity (1500m/sec) pockets to the original SEG/EAGE velocity model. 5Hz Ricker wavelet was used for both the synthetic seismograms and FWI. Inline and crossline shot spacings are 400m in the synthetic seismograms. Figure 3(a) is the true velocity. Figure 3(b) and 3(d) are initial velocities produced by smoothing the true velocity with 2km*4km and 500m*500m moving Gaussian weighting windows. Figure 3(c) and 3(e) are the FWI results from the initial velocities in Figure 3(b) and 3(d), respectively. In Figure 3(c) and 3(e), the shallow velocity anomalies and top of salt are reconstructed well. However, the bottom of salt and intra-salt are not resolved well when the FWI initial velocity is not close to the exact velocity. This result shows that restoring velocities of intra-salt and bottom of salt is challenging in FWI.

To investigate how our FWI algorithm works for data generated by a different propagator and variable density model, we tested BP 2004 velocity benchmark original data generated by Billette and Brandsberg-Dahl (2005). In FWI, the forward modeling was done using 5Hz Ricker source wavelet. Figure 4(a) and 4(b) are true velocity and the initial velocity made by smoothing the true velocity with a 3km*6km moving Gaussian weighting window. Figure 4(c) is the velocity obtained by FWI. Shallow velocity anomalies, shallow sediment velocity and top of salt have been resolved well. However, velocities in bottom of salt and subsalt area were not restored well. Figure 4(d), 4(e) and 4(f) are RTM images in the area shown as the white dash box in Figure 4(a). We can see the improvement in the RTM image using FWI velocity.

Figure 5 are FWI results using a sequence of 3D marine streamer data. Figure 5(a) and 5(b) are initial and FWI velocities. Figure 5(c) and 5(d) are RTM images from the initial and FWI velocities. Continuity and focusing have been improved in the image Figure 5(d). However, the solution is low and needs to be improved.

Conclusion

We improved time domain FWI using source wavelet convolution to field data, windowed back propagation and gradient scaling with square of source side illumination. Our time domain FWI showed promising results in restoring migration velocities in the shallow areas and top of salt. However, velocity reconstruction in the salt and bottom of salt are still challenging in FWI.

Acknowledgements

We thank BP and SEG/EAGE for the synthetic data. We thank TGS for the permission to publish this study.

DOI http://dx.doi.org/10.1190/segam2012-1535.1

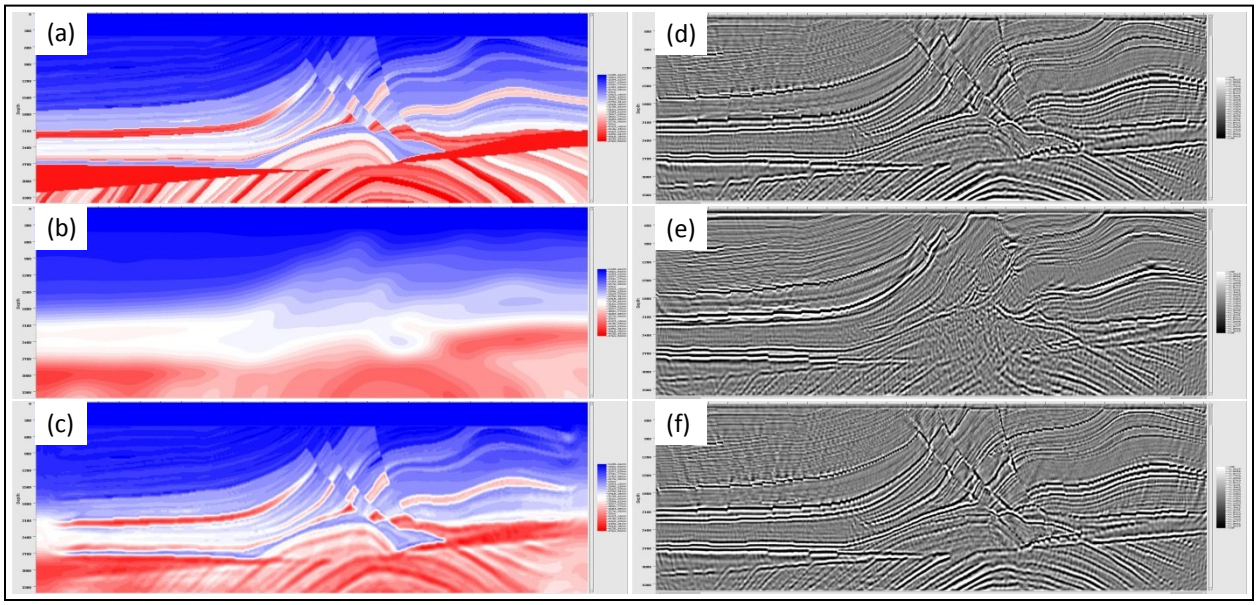

Figure 2. (a) Marmousi 2 velocity model, (b) initial and (c) final FWI velocities. (d), (e) and (f) are RTM images using the velocities of (a), (b) and (c), respectively.

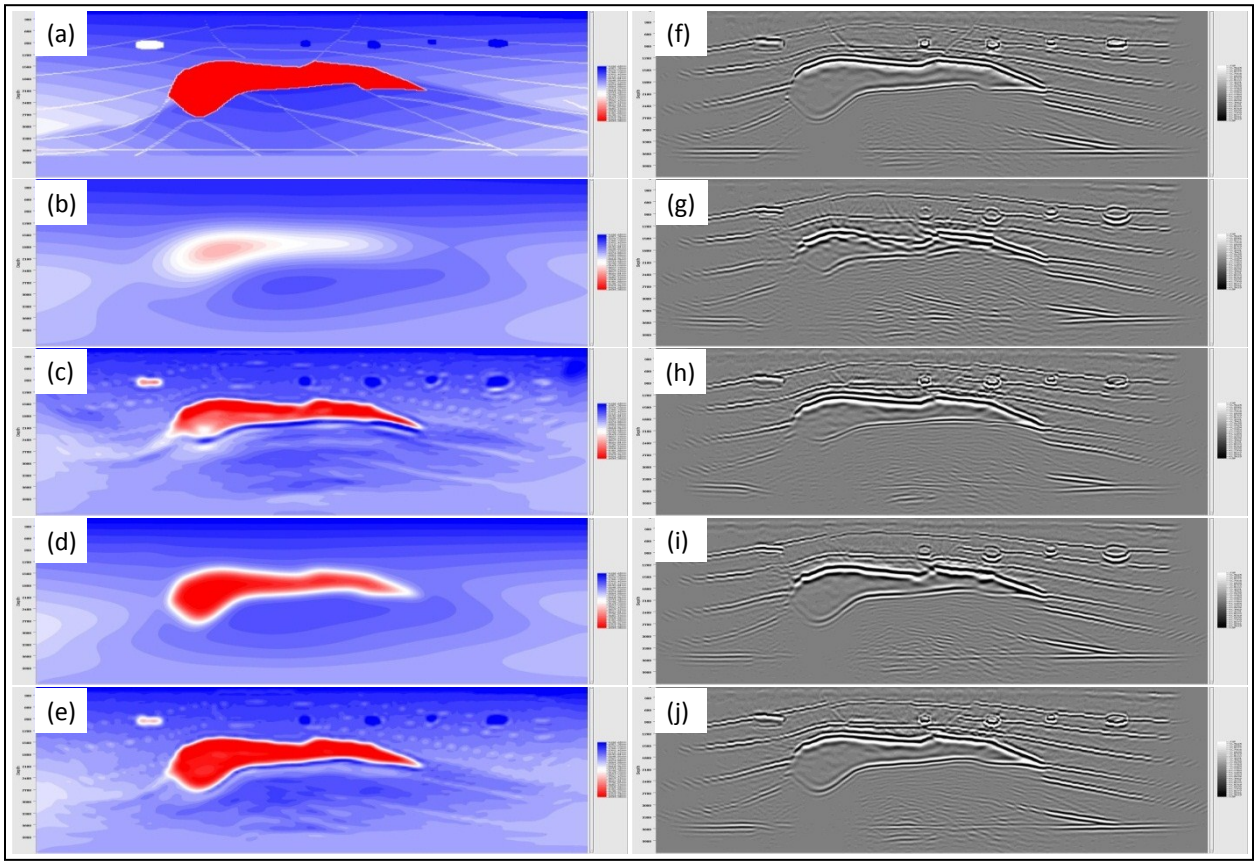

Figure 3. (a) Modified 3D SEG/EAGE model. (b) and (d) are initial models for FWI. (c) and (e) are FWI velocity starting from the velocities in Figure 3(b) and 3(d), respectively. (f), (g), (h), (i) and (j) are RTM images using velocities in Figure 3(a), 3(b), 3(c), 3(d) and 3(e), respectively.

DOI http://dx.doi.org/10.1190/segam2012-1535.1

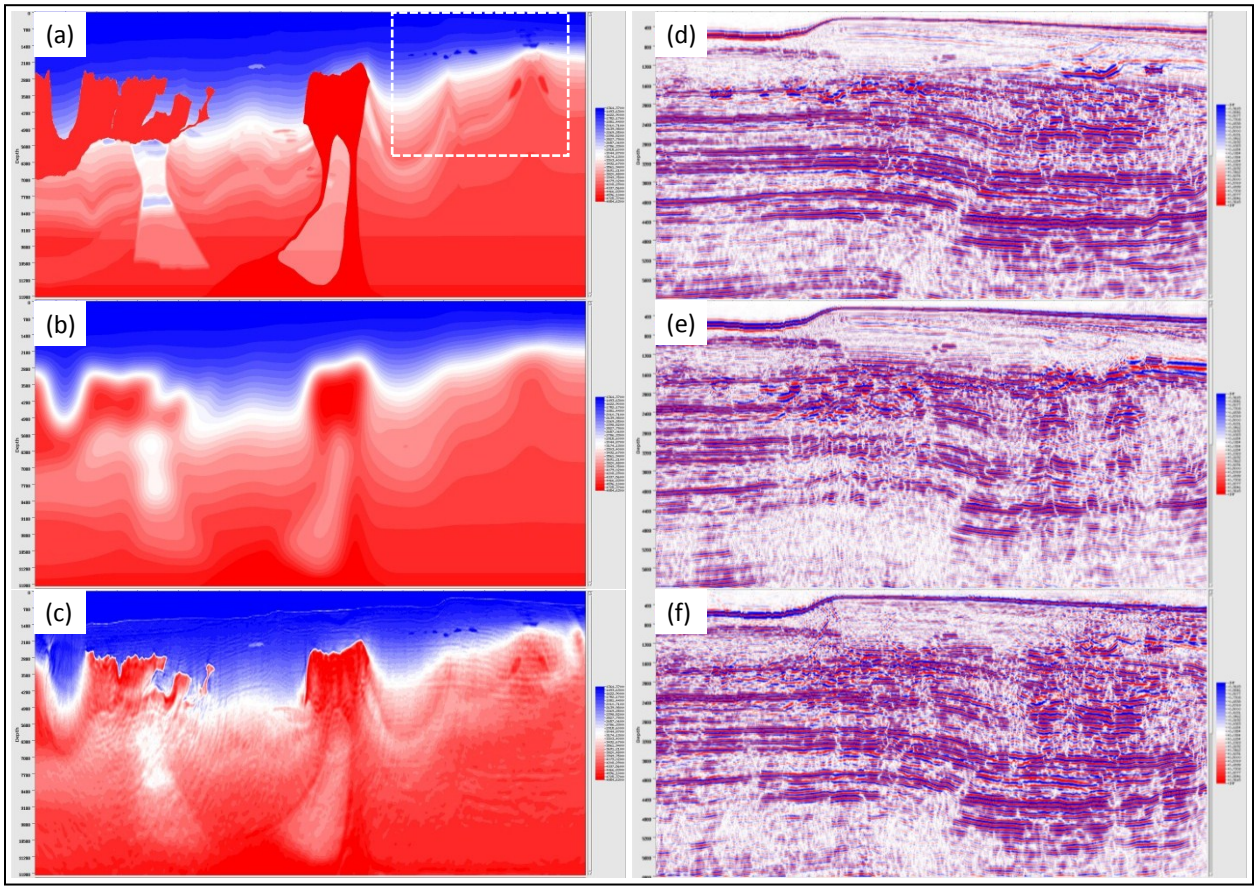

Figure 4. (a) BP2004 velocity model. (b) Initial velocity produced by smoothing the exact velocity with 3km*6km moving Gaussian weighting window. (c) velocity generated by FWI. (d), (e) and (f) are RTM images in the white dash box in Figure 4(a) using the velocities in (a), (b) and (c), respectively.

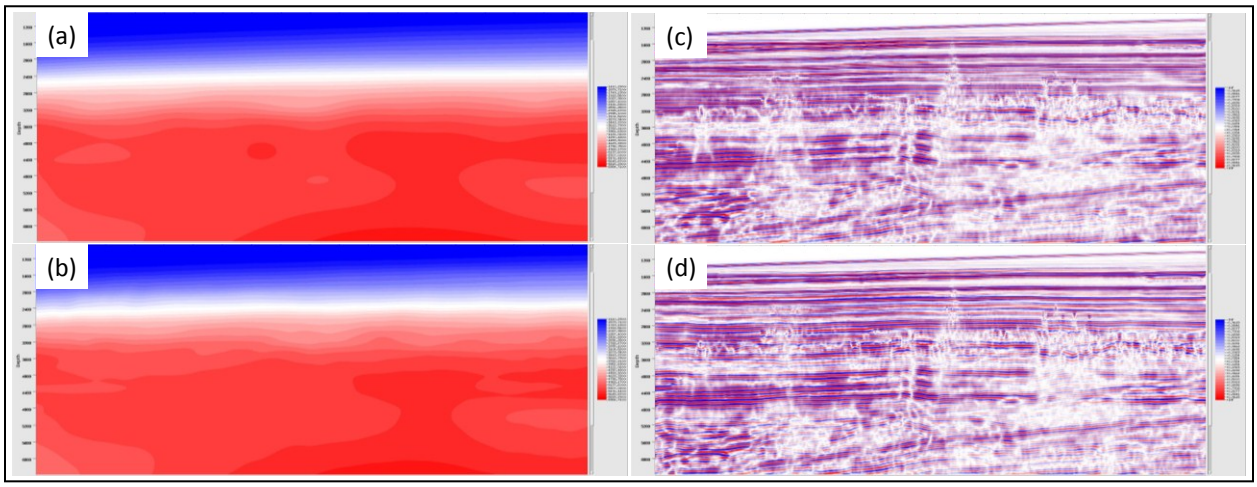

Figure 5. (a) Initial and (b) FWI velocities of 3D marine streamer data. (c) and (d) are RTM images using the velocities in Figure 5(a) and 5(b).

DOI http://dx.doi.org/10.1190/segam2012-1535.1

http://dx.doi.org/10.1190/segam2012-1535.1

EDITED REFERENCES

Note: This reference list is a copy-edited version of the reference list submitted by the author. Reference lists for the 2012 SEG Technical Program Expanded Abstracts have been copy edited so that references provided with the online metadata for each paper will achieve a high degree of linking to cited sources that appear on the Web.

REFERENCES

Billette, F. J., and S. Brandsberg-Dahl, 2005, The 2004 BP velocity benchmark: 67th Conference and Exhibition, EAGE, Extended Abstracts, B035.

Bunks, C., F. Saleck, S. Zaleski, and G. Chavent, 1995, Multiscale seismic waveform inversion: Geophysics, **60**, 1457–1473.

Lazaratos, S., I. Chikichev, and K. Wang, 2011, Improving the convergence rate of full wavefield inversion using spectral shaping: 81st Annual International Meeting, SEG, Expanded Abstracts, 2428–2432.

Martin, G. S., 2004, The Marmousi 2 model, elastic synthetic data and an analysis of imaging and AVO in a structurally complex environment: M.S. thesis, University of Houston.

Pratt, R. G., C. Shin, and G. J. Hicks, 1998, Gauss-Newton and full Newton methods in frequency domain seismic waveform inversion; Geophysical Journal International, **133**, 341–362.

Sirgue, L., B. Denel, and F. Gao, 2011, Integrating 3D full waveform inversion into depth imaging projects: 81st Annual International Meeting, SEG, Expanded Abstracts, 2354–2358.

Tarantola, A., 1984, Inversion of seismic reflection data in the acoustic approximation: Geophysics, **49**, 1259–1266.

Yoon, K., C. Shin, and K. J. Marfurt, 2003, Waveform inversion using time-windowed back propagation: 73rd Annual International Meeting, SEG, Expanded Abstracts, 690–693.